

## Points, Walls, and Loops in Resonant Oscillatory Media

Tetsuya Kawagishi, Tsuyosi Mizuguchi, and Masaki Sano

*Research Institute of Electrical Communication, Tohoku University, Sendai 980, Japan*

(Received 15 February 1995)

In an experimental investigation of oscillatory media, domains and walls are formed under parametric forcing with a frequency double the natural one. In this bistable system, a nonequilibrium transition from an Ising wall to a Bloch wall consistent with prediction is confirmed. The Bloch wall moves in the direction determined by its chirality with a constant speed. A new type of moving structure in two dimensions, a traveling loop consisting of two walls and Néel points, is observed.

PACS numbers: 82.40.Bj, 05.45.+b, 47.20.Ky

Oscillatory media spontaneously form in a wide variety of systems as they are driven away from equilibrium. Examples are seen in many different fields [1–3]. In nonlinear oscillators having a small number of degrees of freedom, one of the central problems is to clarify the ideas of synchronization and resonance. However, despite theoretical and experimental progress, relatively little is known about the response to an external periodic forcing of spatially coupled oscillators. The simplest unresolved case is that of parametric forcing of a system in which nontrivial domain walls are predicted to exist [4]. When the external forcing has a frequency double the natural frequency, two locked states are possible. A domain wall appears between two different locked states formed in this way. In this system, sustained wall motion, including translational and oscillatory motion, is predicted due to the nonvariational effect [4–6], even when two domains are symmetric. This is the crucial difference between domain walls in the systems considered here and those in equilibrium systems whose dynamics are simply relaxational processes governed by the free energy. We present an experimental investigation of parametrically forced oscillatory media. A structural transition of domain walls associated with chirality breaking is elucidated. Furthermore, traveling loops consisting of two types of Bloch walls and Néel points are observed.

Oscillatory media are realized by convective cellular structures referred to as oscillating grid patterns (OGP's) [7] in liquid crystal convection [8]. We used a nematic liquid crystal 4-methoxybenzyliden-4'-butylaniline (MBBA) doped with a 0.01 wt% ion impurity, tetra-*n*-butylammonium bromide, to control the electrical conductivity. This liquid crystal is filled in a cell (2 cm × 2 cm × 50 μm) sandwiched between transparent electrodes. The temperature of the cell is controlled at 25 ± 0.01 °C. Applying an alternating (ac) voltage  $V \sim 60$  V with frequency  $\omega/2\pi \sim 900$  Hz, we obtained a stationary grid pattern (GP). This pattern gives rise to a two-dimensional lattice of about 400 × 400 rectangular convective cells. The nematic directors are stationary since the relaxation time is much longer (about 0.2 sec) than the period of the external ac field [8]. This system

is imaged using a shadowgraph under a microscope with polarized light. The shadowgraphic image intensity is directly related to the orientation of molecules of nematics. In this pattern, sinks and sources form the centered rectangular net, as shown in Fig. 1(a). A slight increase of the voltage causes an oscillatory instability of the grid pattern with natural frequency  $\omega_0$ ;  $\omega_0/2\pi \sim 1.3$  Hz, which is independent of the external frequency  $\omega$ . We call this pattern an OGP, reflecting the fact that the positions of sinks and sources oscillate. This is a good candidate for two-dimensionally distributed oscillatory media.

To observe behavior induced by the parametric forcing of the oscillator lattice, we modulated the ac voltage at nearly double the natural frequency,  $V_m = 2\sqrt{2}V(1 + r \cos \omega_e t) \cos \omega t$ , where  $r$  is the modulation ratio and  $\omega_e = 2\omega_0 + \Delta\omega$ , with the detuning  $\Delta\omega$  small. Here the ac voltage for convection was fixed at  $\omega/2\pi = 928$  Hz and  $V = 66.3$  V, placing the system slightly above the oscillatory instability threshold of the GP [ $\mu \equiv (V - V_c)/V_c = 0.009 \pm 0.001$ , where  $V_c$  is the critical voltage for a Hopf bifurcation]. Typical patterns observed in a phase locked state under parametric forcing are shown in Figs. 1(b) and 1(c). The dark lines are interfaces between two phase locked states. Across the dark lines the phase of the oscillation jumps by  $\pi$ , as will be shown later. These interfaces are walls in dynamical systems. Unlike in equilibrium systems, these walls can exhibit transitions from stationary to propagating states by varying the control parameters  $r$  and  $\omega_e$ . We show the phase diagram corresponding to these parameters in Fig. 2(a). In the right half of the phase locked region, the wall exhibits stationary spatial periodic patterns (stripes) as shown in Fig. 1(c). As we decrease the modulation frequency, the wavelength of the pattern increases, finally resulting in isolated walls in the left half of the phase locked region as shown in Fig. 1(b). The transition from stripes to isolated walls seems to be a second order transition. Detailed results concerning this point will be presented elsewhere [10]. Here we focus on the region in which stationary or propagating isolated walls are observed. To elucidate the transition from stationary to propagating walls, we measured the velocity of the moving wall as a function of

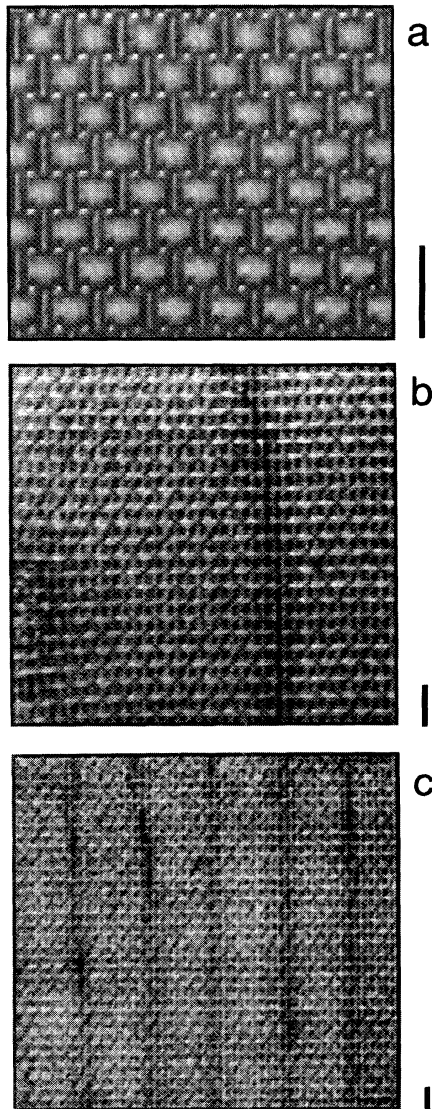


FIG. 1. A shadowgraphic image of the grid pattern. The length of the accompanying bars corresponds to  $100 \mu\text{m}$ . (a) A snapshot of an oscillating grid pattern (OGP). (b) An OGP under parametric forcing. Dark lines are domain walls between two different locked states. (c) Same as (b) but showing stripe pattern.

modulation frequency  $\Delta\omega$  [Fig. 2(b)], while fixing  $r = 0.13$  [Fig. 2(b)]. The results indicate that the transition is second order consistent with prediction [4].

It was predicted that the spontaneous breaking of chirality is responsible for the transition from stationary to moving walls in nonequilibrium systems [4]. These stationary walls are referred to as Ising walls and the moving ones as Bloch walls, employing an analogy to the anisotropic  $X$ - $Y$  model [9]. If the observed stationary interfaces are Ising walls, the amplitude of oscillation must vanish where the phase jumps. If the moving interfaces are Bloch walls, the amplitude does not vanish at the core, but rather two domains are connected by rotating the vector of the com-

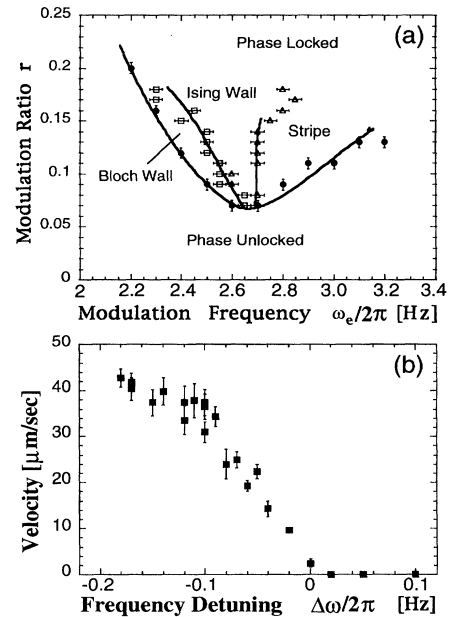


FIG. 2. (a) The phase diagram of the parametric forcing as a function of modulating ratio  $r$  and frequency  $\omega_e$ . (b) Traveling velocity of Ising and Bloch walls as a function of frequency detuning  $\Delta\omega$  with fixed  $r = 0.13$ .

plex order parameter of the oscillation. The chirality of the wall is defined by the direction of this rotation, i.e., right handed or left handed [4]. The direction of motion of the wall is determined by the chirality. Hence one can judge wall types by their amplitude at the core and chirality.

In order to clarify the structural transitions of walls, we perform the following analysis. The image intensity  $\mathcal{G}(x, y, t)$  was digitized with a resolution of  $640 \times 480$  pixels and 256 grey scale levels at a frequency of 15 Hz. Here we choose the  $x$  axis to be parallel to the direction of the alignment of nematics.

Under parametric forcing, the OGP has a natural temporal frequency  $\omega_0$  (1.25 Hz) and lattice wave number  $(k_x, k_y) = (2\pi/63, 2\pi/105) \mu\text{m}^{-1}$ . Thus at the lowest order one can expand  $\mathcal{G}(x, y, t)$  as

$$\mathcal{G}(x, y, t) = [1 + a \exp(i(\omega_0 t + \psi))] \exp(ik_x x + ik_y y) + \text{c.c.} + \text{h.o.t.}, \quad (1)$$

where  $a$  represents the amplitude,  $\psi$  the phase of the oscillation mode, and h.o.t. denotes higher order terms. This amplitude and phase are slowly varying functions in space and time compared with the lattice wave number and natural frequency. In order to obtain only the slow variations in Eq. (1), we used a broadband pass filter centered at  $\omega_0$  in frequency and  $(k_x, k_y)$  in wave number. Thus we obtained a filtered signal  $a \exp(i\psi)$ , which is the complex order parameter of our system.

Although the oscillation and interfaces are two-dimensional phenomena, to see temporal evolution of interfaces clearly first we show a profile of the amplitude field  $a$  along a line intersecting a wall perpendicularly.

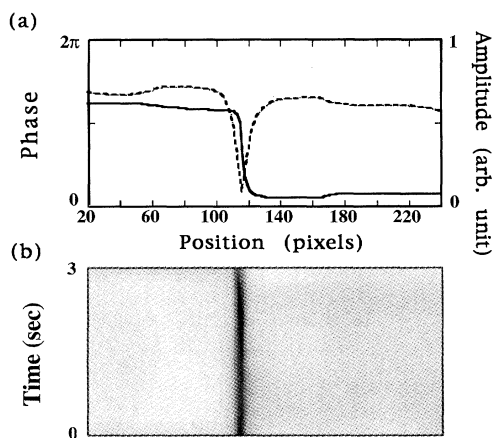


FIG. 3. The profile of a stationary interface along a line intersecting a wall. (a) The spatial variation of the amplitude (dotted line) and the phase (solid line). (b) Space-time evolution of the amplitude profile. Black (white) pixels correspond to a small (large) amplitude of oscillation.

Figure 3 depicts the results for a stationary wall. In Fig. 3(a), the solid line represents the spatial variation of the phase. It is apparent that there is a sharp change of  $\pi$  in the phase near the center of the wall. Correspondingly, the amplitude (dotted line) falls almost to zero. A spatiotemporal plot of the amplitude profile in Fig. 3(b) shows clearly that the wall is stationary. Therefore we conclude that stationary walls are Ising walls. On the other hand, in Fig. 4 we exhibit the results for a moving wall. The amplitude at the wall is relatively small but does not vanish [dotted line in Fig. 4(a)]. The phase gradually changes by  $\pi$  at the center of the wall [solid line in Fig. 4(a)]. Notice that the slope of this curve is less steep than in the case of the Ising wall. Also note that the wall is moving to the left, as depicted in the spatiotemporal plot of the phase profile [Fig. 4(b)]. Consequently, it is concluded that moving walls are Bloch

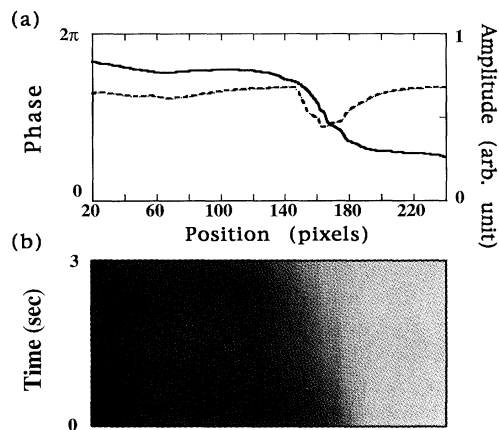


FIG. 4. The profile of a moving interface along a line intersecting a wall. (a) The spatial variation of the amplitude (dotted line) and the phase (solid line). (b) Space-time evolution of the phase variation. The grey scale corresponds to 0 for white and  $2\pi$  for black.

walls. As in easy-axis ferromagnets, there are two kinds of Bloch walls in this system. The phase decreases from the left domain to the right domain in Fig. 4. The other kind of Bloch walls, exhibiting rightward motion, were also observed. These walls connect the same type of domains, but with increasing phase. Hence the motion of Bloch walls is determined by their chirality.

Let us now discuss two-dimensional structures and behavior. In two dimensions, Bloch walls can form closed loops. The simplest loop is one consisting of only a single type of Bloch wall which expands, invading the outer region, or shrinks, invading the inner region. This distinction depends on the loop's chirality [see Figs. 5(a) and 5(b)]. However, interesting motion is expected if the loop consists of two different types of Bloch walls joined at two points [Fig. 5(c)]. Such a point is called a Néel point or connecting point (CP) [12,14]. Some interesting phenomena are expected to result from the interplay between two types of Bloch walls joined at a CP. As one such phenomenon, we report a new type of moving structure in two-dimensional space, translational motion of a loop. Figure 6(a) shows a snapshot of a moving loop exhibiting translational motion to the right. The loop travels persistently in one direction until it collides with other walls or loops. We analyzed the two-dimensionally distributed oscillators near the upper end of the loop. Figure 6(b) shows the spatial phase variation. It is seen that two different Bloch walls are connected at a kind of branch cut of a  $2\pi$  jump. In Fig. 6, the left and right domains are the same, since they are connected outside the loop. The branch cut results from this fact. Notice that the center domain is connected to the right one by increasing the phase and to the left one by decreasing the phase. An increase and decrease in the phase correspond to left- and right-handed rotations of the vector of the complex order parameter. The directions of the wall's motions are opposite to each other, i.e., one invades outward and the other inward. Hence again the motion of the Bloch wall is determined uniquely by its chirality. Considering the topology of the loop, two CP's must exist at the upper and lower ends of the loop, which correspond to the singular points of the branch cut. The amplitude of a single type of

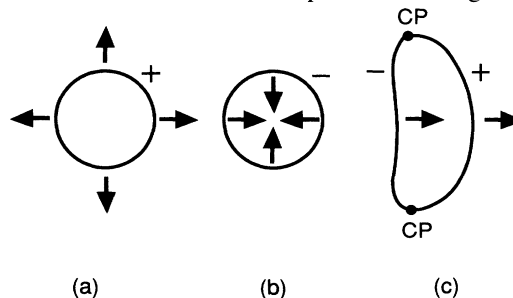


FIG. 5. Schematic illustration of possible types of loops. (a) An expanding loop consists of a Bloch wall (+). (b) A shrinking loop consists of a Bloch wall (-). (c) A traveling loop consists of two Bloch walls (+ and -) and Néel points (CP's).

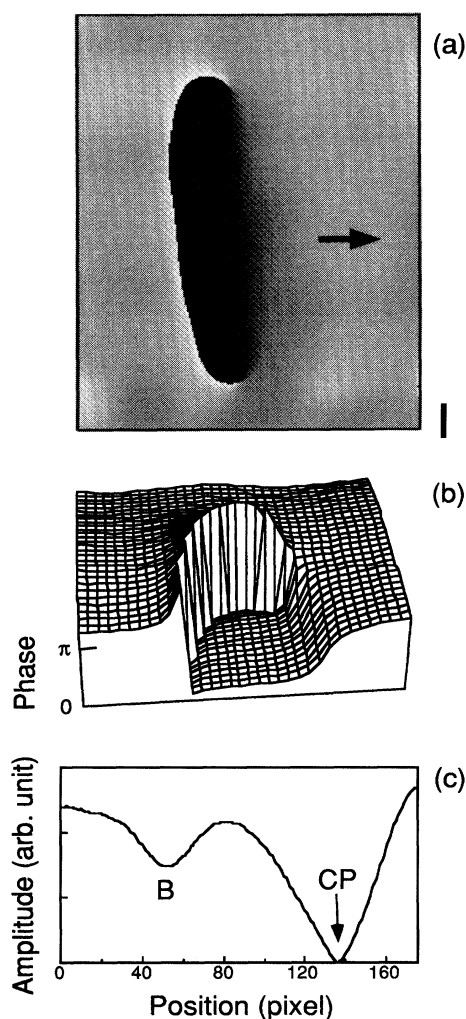


FIG. 6. Experimental data of a traveling loop. (a) Phase distribution of a snapshot of a loop exhibiting translational motion to the right. The bar corresponds to  $100 \mu\text{m}$ . (b) Spatial variation of the phase around the upper end of the loop. (c) Cross section of an amplitude profile which crosses a Bloch wall (B) and a CP. The amplitude vanishes at the CP.

Bloch wall does not vanish, but in the case of two different Bloch walls joined at a CP the amplitude must vanish at the CP due to a topological constraint. We plot the cross section of the amplitude profile crossing interfaces twice, one at a Bloch wall and one at a CP in Fig. 6(c). Figure 6(c) shows that the amplitude is relatively small at the Bloch wall and zero at the CP. This confirms that the traveling loop consists of two different types of Bloch walls and two CP's, as schematically illustrated in Fig. 5(c).

In traveling loops, CP's move with the Bloch walls. This is in contrast with usual spiral patterns in which the core (CP) remains stationary [11–13]. A possible reason for this is the following. In the present experiment, the system is fully nonvariational because the system consists

of limit cycle oscillators. In fact, the traveling loop can be observed numerically in the complex Ginzburg-Landau (CGL) equation with a parametric forcing term by an appropriate choice of the linear dispersion coefficient and the detuning parameter [14]. Recently observed traveling spots in a model reaction diffusion equation [15] seem very similar to the present traveling loops. Therefore we believe that the phenomena are generic in (resonant) oscillatory media. The mechanism of the motion of CP may be related to core meandering in spiral patterns. This is an open problem in resonant systems. Understanding the motion of the loops and connecting points pose interesting problems about dynamics of interfaces: walls, lines, and points appearing in higher-dimensional space for nonequilibrium systems [16].

We thank Y. Sawada, Y. Kuramoto, S. Sasa, and H. Sakaguchi for valuable discussions, and H. Kokubo for helpful suggestions on the experiment.

- 
- [1] J. M. Flesselles, V. Croquette, and S. Jucquois, *Phys. Rev. Lett.* **72**, 2871 (1994); M. Sano, K. Sato, and S. Nasuno (to be published).
  - [2] G. S. Skinner and H. L. Swinney, *Physica (Amsterdam)* **48D**, 1 (1991).
  - [3] M. Courtemanche, L. Glass, and J. P. Keener, *Phys. Rev. Lett.* **70**, 2182 (1993); A. T. Winfree, *When Time Breaks Down* (Princeton Univ. Press, Princeton, 1987).
  - [4] P. Couillet, J. Lega, B. Houchmanzadeh, and J. Lajzerowicz, *Phys. Rev. Lett.* **65**, 1352 (1990); P. Couillet, J. Lega, and Y. Pomeau, *Europhys. Lett.* **15**, 221 (1991).
  - [5] T. Mizuguchi and S. Sasa, *Prog. Theor. Phys.* **89**, 599 (1993).
  - [6] A. Hagberg and E. Meron, *Phys. Rev. E* **48**, 705 (1993).
  - [7] M. Sano, H. Kokubo, B. Jانياud, and K. Sato, *Prog. Theor. Phys.* **90**, 1 (1993).
  - [8] P. G. de Gennes, *The Physics of Liquid Crystals* (Clarendon Press, Oxford, 1974).
  - [9] J. Lajzerowicz and J. J. Niez, *J. Phys. (Paris) Lett.* **40**, L-165 (1979).
  - [10] H. Riecke, J. Crawford, and E. Knobloch, *Phys. Rev. Lett.* **61**, 1942 (1988); H. Riecke, M. Silber, and L. Kramer, *Phys. Rev. E* **49**, 4100 (1994); D. Walgraef, *Europhys. Lett.* **7**, 495 (1988); P. Couillet and K. Emilsson, *Physica (Amsterdam)* **61D**, 119 (1992).
  - [11] K. B. Migler and R. B. Meyer, *Phys. Rev. Lett.* **66**, 1485 (1991); *Phys. Rev. E* **48**, 1218 (1993).
  - [12] T. Frish, S. Rica, P. Couillet, and J. M. Gilli, *Phys. Rev. Lett.* **72**, 1471 (1994).
  - [13] S. Nasuno, N. Yoshimo, and S. Kai (to be published).
  - [14] S. Sasa, T. Mizuguchi, and M. Sano, in *Spatio-temporal Patterns in Nonequilibrium Complex Systems*, edited by P. E. Cladis and P. Palfy-Muboray (Addison-Wesley, Reading, 1995), pp. 331–342.
  - [15] K. Krischer and A. Mikhailov, *Phys. Rev. Lett.* **73**, 3165 (1994).
  - [16] M. Kleman, *Points, Lines and Walls* (John Wiley Sons, New York, 1983).

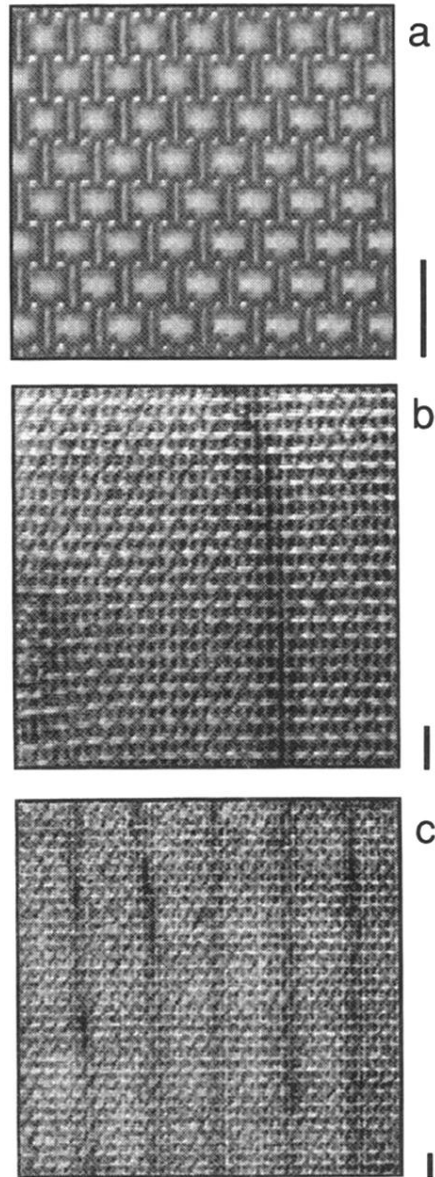


FIG. 1. A shadowgraphic image of the grid pattern. The length of the accompanying bars corresponds to  $100\ \mu\text{m}$ . (a) A snapshot of an oscillating grid pattern (OGP). (b) An OGP under parametric forcing. Dark lines are domain walls between two different locked states. (c) Same as (b) but showing stripe pattern.

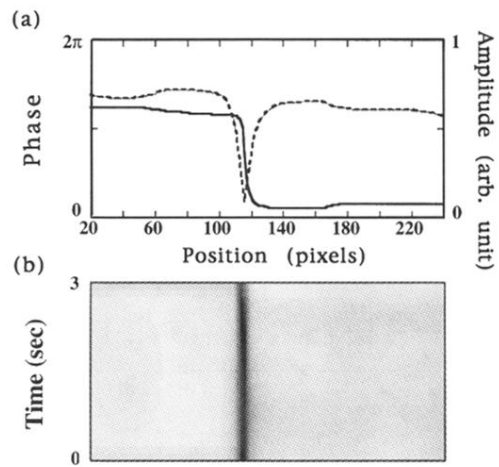


FIG. 3. The profile of a stationary interface along a line intersecting a wall. (a) The spatial variation of the amplitude (dotted line) and the phase (solid line). (b) Space-time evolution of the amplitude profile. Black (white) pixels correspond to a small (large) amplitude of oscillation.

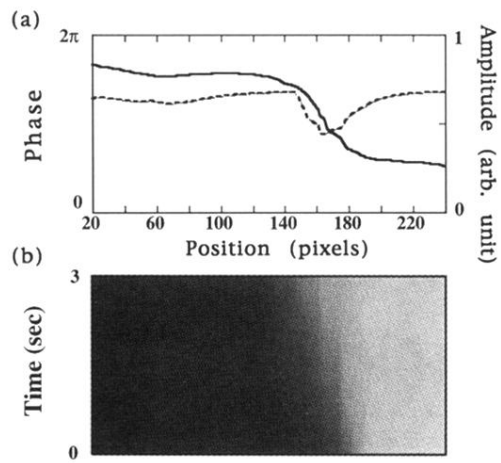


FIG. 4. The profile of a moving interface along a line intersecting a wall. (a) The spatial variation of the amplitude (dotted line) and the phase (solid line). (b) Space-time evolution of the phase variation. The grey scale corresponds to 0 for white and  $2\pi$  for black.

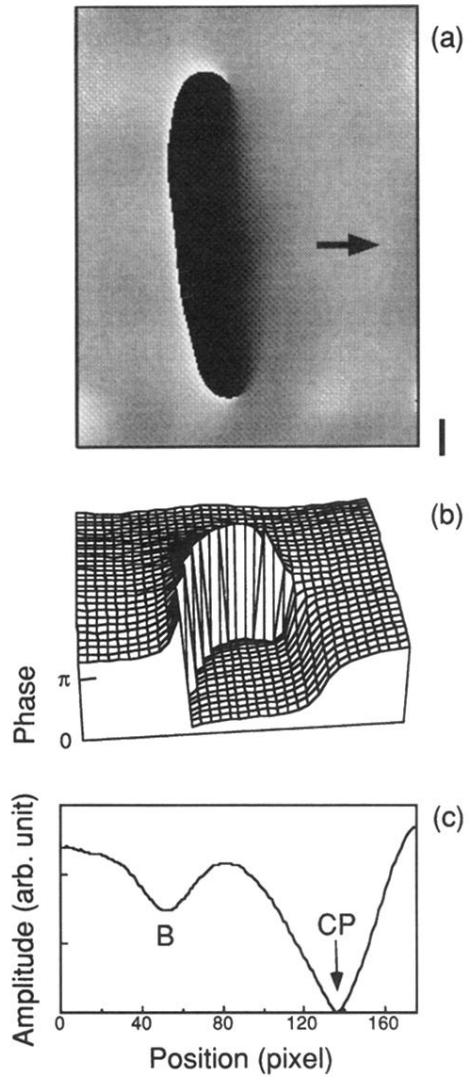


FIG. 6. Experimental data of a traveling loop. (a) Phase distribution of a snapshot of a loop exhibiting translational motion to the right. The bar corresponds to  $100 \mu\text{m}$ . (b) Spatial variation of the phase around the upper end of the loop. (c) Cross section of an amplitude profile which crosses a Bloch wall (B) and a CP. The amplitude vanishes at the CP.